

We are IntechOpen, the world's leading publisher of Open Access books Built by scientists, for scientists

6,900

Open access books available

186,000

International authors and editors

200M

Downloads

Our authors are among the

154

Countries delivered to

TOP 1%

most cited scientists

12.2%

Contributors from top 500 universities



WEB OF SCIENCE™

Selection of our books indexed in the Book Citation Index
in Web of Science™ Core Collection (BKCI)

Interested in publishing with us?
Contact book.department@intechopen.com

Numbers displayed above are based on latest data collected.
For more information visit www.intechopen.com



Release Profile of Nitrogen during Thermal Treatment of Waste Wooden Packaging Materials

Liuming Song, Xiao Ge, Xueyong Ren, Wenliang Wang, Jianmin Chang and Jinsheng Gou

Abstract

In this paper, the fast pyrolysis experiment of particle board was carried out on a fixed bed reactor and a Py-GC/MS equipment. The effects of temperature and gas phase residence time on the product yields and its components distribution were investigated. The effect of components of particle board on product yields and its components distribution was also investigated. The results showed that the temperature has a great influence on the yields of fast pyrolysis products, and the yield of pyrolysis oil reached the highest at 550°C. The urea-formaldehyde resin would prevent the pyrolysis of particle board. Compared with the bio-oil from fast pyrolysis of wood, the major components of the bio-oil from fast pyrolysis of particle board did not change much.

Keywords: pyrolysis, fixed bed, Py-GC/MS, particle board, bio-oil

1. Introduction

The world concerns about environmental pollution caused by fossil fuel combustion and exhaustion of energy resources have drawn significant attention to researchers. Biomass can be converted into various fuels and chemicals by different methods to replace petrochemical fuels [1–3]. Fast pyrolysis of biomass is one of the most promising and fast developing biomass thermochemical conversion technologies, which can turn organic materials into high value products such as chemical products or liquid fuels. And this technology has been widely used in the field of biomass renewable utilization in recent years [4–6]. This transformation into an environment-friendly renewable energy sources can replace the fossil fuels consumed and reduce greenhouse gas emissions. Among the biomass, the large amount of waste wood has attracted increasing attention because it can be used as an energy and reduce the waste of timber [7–9].

Particle boards occupy a large proportion of waste wood, so how to effectively convert it into high value chemical products has attracted the attention of researchers. Choi et al. [3] conducted fast pyrolysis of particle board over three types of zeolite catalysts, the results showed that the bio-oil yield and gas yield in catalytic pyrolysis was lower and higher than those in non-catalytic pyrolysis, respectively. Park et al. [10] also examined the catalytic pyrolysis of particle board using a nanoporous catalyst and showed that bio-oil is composed mainly of

oxygenates, phenolics and acids, with smaller amounts of aromatics and hydrocarbons. Lee et al. [11] investigated the co-pyrolysis of waste particle board and polypropylene over four types of catalysts, they found that catalytic co-pyrolysis suppressed the formation of PAHs, and the quality of bio-oil has improved. When the particle board was combined with other materials for co-pyrolysis, or when the particle board was pyrolyzed over different catalysts, high quality bio-oil or aromatic products could be obtained [8, 11–13].

When only the particle board was pyrolyzed, many researchers have found that temperature was the most important factor to determine the yields of bio-oil and gas products. Most scholars have only studied the influence of temperature on the pyrolysis characteristics of wood and particleboard, and there are few literatures concerning the influence of other conditions on the pyrolysis characteristics of wood and particle board. In this paper, fast pyrolysis experiments were carried out in fixed bed reactor and a Py-GC/MS equipment, and the effects of temperature and gas phase residence time on the product yields and its components distribution were investigated. The effect of components of particle board on product yields and its components distribution was also investigated.

2. Materials and methods

2.1 Experimental materials and characteristics analysis

2.1.1 Experimental materials

The experimental samples selected for this study included two types of solid wood, a wood adhesive, and six types of particle board.

Two types of solid wood, Larch wood (*Larix gmelinii* (Rupr.) Rupr.) and Poplar wood (*Populus deltoides*), which are the most commonly used for the production of wood based panel, were selected. Larch wood and Poplar wood were obtained from the north of Daxinganling, Inner Mongolia, the age of the trees was around 30 and 10 years respectively. Larch wood and Poplar wood were marked with “Larch” and “Poplar” respectively.

Urea formaldehyde (UF) is the most commonly used adhesive in the wood based panel industry. Provided by Beijing Taier Chemical Co., Ltd., its F/U molar ratio is 1.1 and the solids content is 53%.

PBL: Larch Particle Board and PBP: Poplar Particle Board. The adhesive levels used for preparing particle boards were 5%, 10%, and 20%, respectively.

The particle board was made in our laboratory (width: 400 × 400 mm, thickness: 10mm). There was a certain difference between self-made particle board and actual waste particle board, but there were uncertainties in the waste time, wood types, adhesive types and content, etc., which were actually unfavorable for research and analysis of results. Therefore, the particle board was placed in a room under controlled environment for 6 months after preparation to simulate the waste particle board in nature.

2.1.2 Characteristic analysis

The materials of solid wood and particle board were crushed, sieved and dried before the experiment. After the adhesive was dried and solidified in the oven, it was crushed and sieved, all materials have a particle size of about 1 mm. Elemental analysis, industrial analysis and component analysis of raw materials are shown in **Tables 1–3**, respectively.

Sample ^a	C%	H%	O% ^b	N%
Larch	46.15	6.31	47.36	0.12
Poplar	45.24	6.30	48.36	0.10
UF	33.45	5.02	29.31	32.22
PBL (10% sizing amount)	44.15	6.11	46.28	3.46
PBP (10% sizing amount)	43.35	5.96	47.55	3.14

^aThe test result was an air-drying base.

^bThe oxygen value was obtained by subtraction.

Table 1.
Element analysis of samples (wt%).

Sample ^a	M%	A%	V%	FC%
Larch	7.26	1.78	73.12	17.84
Poplar	6.79	1.81	72.51	18.89
UF	2.18	0.53	95.98	1.31
PBL	6.04	1.68	73.43	18.85
PBP	6.37	1.57	73.01	19.05

^aThe test result was an air-drying base.

Table 2.
Proximate analysis of samples (wt%).

Sample ^a	Cellulose %	Hemicellulose % ^b	Holocellulose %	Lignin %	pH	Ash %	Benzol extractive %
Larch	42.76	20.79	63.55	24.03	4.90	0.905	3.26
Poplar	45.87	28.44	74.31	19.12	5.01	1.169	5.89

^aThe test result was an air-drying base

^bThe hemicellulose value was obtained by subtraction.

Table 3.
Component analysis of samples.

Elemental analysis of raw materials was performed using the VarioEL elemental analyzer at the Analytical Center of Changchun Institute of Chemicals, Chinese Academy of Sciences. The analysis was conducted in accordance with the International “Method for Analysis of Carbon, Hydrogen, and Oxygen in Rock Organic Matter” (GB/T 19143-2003), where C, H, and N elements were tested experimentally and the final results were averaged twice for the experiment. The O element content was obtained by subtraction.

The industrial analysis was completed at the Chemical Laboratory of Beijing Forestry University, and conducted according to the national standard “Test Methods for Charcoal and Charcoal” (GB/T17664-1999). From **Table 2**, it can be concluded that the ash content of Poplar was larger than that of Larch, and the volatile content of particle board and solid wood was equivalent, while the volatile content of UF resin was much higher than that of solid wood and particle board, but the fixed carbon of particle board was higher than solid wood and UF resin.

The chemical composition analysis was performed in the Bio-oil Adhesives Laboratory at Beijing Forestry University. The raw material preparation was performed in accordance with the national standard, “Analysis of Samples for Papermaking Raw Material Analysis” (GB/T 2677.1-93). The lignin content was determined according to the national standard “Determination of Acid-insoluble Lignin in Papermaking Raw Materials” (GB/T 2677.8-94), the cellulose content was extracted by nitric acid ethanol method, and the holocellulose content was determined according to the national standard “Determination of Holocellulose Content of Papermaking Raw Materials” (GB/T 2677.10-1995). The lignin content of Larch was higher than that of Poplar from **Table 3**, while the Poplar content of cellulose and hemicellulose was higher than that of Larch.

2.2 Experimental devices and methods

In this article, two devices were used to discuss the fast pyrolysis characteristics of waste particle board. One was a fixed bed fast pyrolysis device (fixed-bed reactor), and the other was a Py-GC/MS equipment. The yields of product were obtained from the fast pyrolysis experiments which were carried out on the fixed bed reactor. The distribution of components in the liquid phase products and the distribution of nitrogen were analyzed by Py-GC/MS equipment.

2.2.1 Fixed bed reactor and experimental method

In this paper, a set of experimental apparatus for fast pyrolysis of small gas entrainment fixed bed was designed, precise automatic temperature control and extremely short gas phase residence time could be achieved through the device. The whole device consisted of gas supply system, sampling system, pyrolysis system, product absorption and measurement system. The schematic diagram of the experimental device is shown in **Figure 1**.

The gas supply system consisted of nitrogen cylinder, flow meter and three-way valve, etc. Nitrogen cylinder was equipped with safety valve and the nitrogen gas purity was 99.999%. The sampling system consisted of a feeding pipeline and a vibrating feeding device, which allows the continuous and

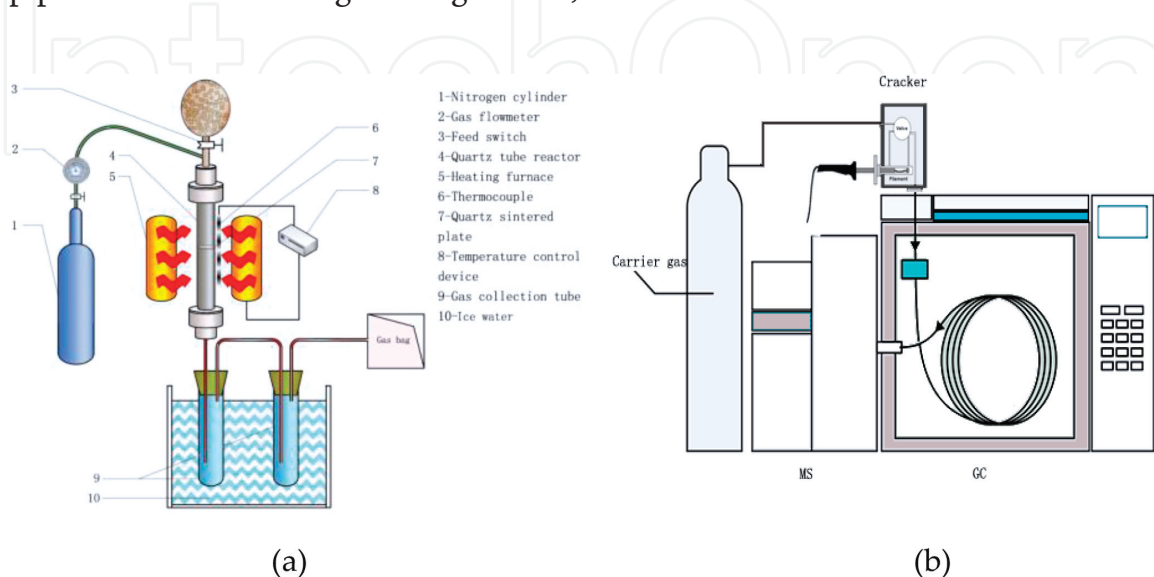


Figure 1. Schematic of (a) fixed bed fast pyrolysis reactor with carry gas feeding module, and (b) Py-GC/MS.

uniform feeding of small amount of materials (less than 5 g). The pyrolysis system consisted of an automatic temperature-controlled electric heating furnace, a quartz tube reactor and a pipe end interface. The fixed-bed reactor was a quartz tube with an inner diameter of 20mm and a length of 500 mm, a quartz sintered plate was set in the middle of the tube to filter pyrolytic carbon produced by pyrolysis, both ends of the quartz tube were special metal quick connectors for convenient installation and removal, connected with stainless steel pipe through quick connector. The product absorption system consisted of a two-stage ice-water bath condensing tube, and an exhaust gas collection bag coupled with a volume flow meter.

The requirement of temperature for fast pyrolysis is 400~600°C [1, 14–15]. In this paper, in order to explore the pyrolysis characteristics of temperature and the nitrogen release mechanism of the particle board, four pyrolysis temperatures were selected, which were 450, 500, 550 and 600°C, respectively.

The requirement for the gas phase residence time of the fast pyrolysis process is 3–0.1 s [1, 14, 15], in order to investigate the influence of gas-phase residence time on the pyrolysis characteristics and nitrogen release mechanism of particle board, three gas-phase residence time were set in the research process, which were 3, 1 and 0.5 s respectively. Considering that the gas phase residence time was controlled by the flow rate of the carrier gas during the actual experiment, the relationship between the gas flow rate and the gas phase residence time at different pyrolysis temperatures was calculated before the formal experiment, the corresponding carrier gas flow rate was 0.1, 0.16, and 0.3 m³/h, respectively.

The temperature of the heating furnace was first determined during the experiment, and the pyrolysis system will stably maintained at the pyrolysis temperatures; then, the prepared feedstock was loaded into the feeding bag; open the intake system valve at a predetermined flow rate and began to purge the entire experimental pipeline with high-purity nitrogen to obtain the inert environment. After the temperature of the pyrolysis system was stabilized to the pyrolysis temperature, the feedstock particle slowly entered the injection line through the vibration feed tube, the material which fell into the injection line entrained by the carrier gas into the quartz tube reactor for fast pyrolysis reactions. The pyrolysis-generated volatiles and pyrolytic carbons entered the gas absorption and metering system with the carrier gas after being filtered by the sintered plate in the center of the quartz tube and the filter quartz wool placed at the end of the reactor pipeline. Pyrolytic carbon remaining in the reactor was collected after pyrolysis was completed.

The calculation of fast pyrolysis gas yield was converted into weight fraction after metering volume by flowmeter, the fast pyrolysis carbon yield was calculated by direct weighing, and the fast pyrolysis oil yield was obtained by subtraction method. In a typical experiment run, the feeding amount was 3 g, and the reaction temperatures of the fixed-bed quartz tube were 450, 500, 550, and 600°C respectively, the carrier gas flow rates were 0.1, 0.16, and 0.3 m³/h respectively, and the pyrolysis time was 5 min.

2.2.2 Pyrolysis gas chromatography combined experimental device and method

The Py-GC/MS equipment included a cracking system and a gas chromatography coupled with mass spectrometry analysis system. The cracking system consisted of a CDS5150 fast thermal cracker, which was equipped with injection and gas loading supply system manufactured by CDS, USA. The gas chromatography

mass spectrometry analysis system consisted of a Shimadzu GCMS-QP2010Plus GC/MS analysis manufactured by Shimadzu Corporation of Japan. The pyrolysis system and the gas chromatograph mass spectrometry system were connected by a special insulation connecting pipeline, the chromatographic column was M-5 ($60\text{ m} \times 0.25\text{ mm} \times 0.25\text{ }\mu\text{m}$). The schematic diagram of the experimental device is shown in **Figure 1**.

During the experiment, accurately weighed raw materials and a little amount of quartz fiber were placed in the quartz tube of the CDS5150 cracker. The pyrolyzer was purged with high-purity nitrogen as the carrier gas, pyrolyzed at the determined heating rate, pyrolysis time, and pyrolysis temperature, and the product was analyzed online by GC/MS. The spectra obtained for each test were analyzed using the system's software. The NIST library was used to record the product's absolute peak area and relative peak area.

When using the NIST library for analysis, most of the peaks could be identified and confirmed, but there were also a small number of peaks that could not be determined (the degree of similarity between the library and the standard material provided by the library was too low). Therefore, the sum of the relative peak area content determined by GC/MS in the relevant experimental results was less than 100%. The part where the sum did not reach 100% was the unknown product, but this part was very small and was represented by other classes in the result analysis.

The Py-GC/MS experimental conditions and instrument parameter settings are shown in **Table 4**.

Parameter name	Setting value	
Cracking conditions	Heating rate	20°C/ms
	Pyrolysis temperature	400, 500, 600°C
	Cracking time	15 s
	Gas flow	100, 50, 10 ml/min
Gas chromatographic conditions	Inlet temperature	280°C
	Gas loading	He
	Gas flow rate	1.0 ml/min
	Split ratio	100:1
	Heating program	50°C constant temperature 5 min, warm up to 280°C at 10°C/min, constant temperature 15 min
	Interface temperature	280°C
	Ion source temperature	250°C
Mass spectrometry conditions	EI source electron energy	70 eV
	Scanning method	SCAN
	Scan range	(20–450) u

Table 4. Conditions and parameters for Py-GC/MS experiments.

3. Results and discussion

3.1 Influence of pyrolysis conditions on the yields of fast pyrolysis product of waste particle board

3.1.1 Effect of temperature on yields of fast pyrolysis product

Figure 2 shows the yields of fast pyrolysis products of UF resin, two types of wood and particle board at different temperatures. As can be seen from the figure, the effect of temperature on the pyrolysis products of raw materials was basically the same in the experimental temperature range. Wood mainly consists of cellulose, hemicellulose and lignin, and therefore its pyrolysis behavior can be considered to be the sum of the behaviors of these three components [16]. The pyrolysis products contain such substances as CO, CO₂, H₂, CH₄, C₂H₄, amine, alcohol, phenol, acid, ketone, sugar, aldehyde, ester, ether, hydrocarbon and heterocyclic. As the temperature rise, the yields of gas product gradually increased, and the rising tendency became more pronounced when the temperature exceeded 550°C. The yields of pyrolytic carbon gradually decreased with the increase of temperature, when the temperature exceeded 550°C, the downward trend tended to be gentle. The yields of pyrolysis oil increased and then decreased with the increase of temperature, which reached a maximum at 550°C. During the pyrolysis process, the carbonization reaction dominated at a lower temperature, and the volatilization was insufficient. At a higher temperature condition, the cracking reaction intensified, a large number of condensable volatiles precipitated, the yield of pyrolysis oil increased subsequently, and the output of pyrolytic carbon decreased. At 600°C, the secondary cracking in the reaction system will gradually strengthen while the components in the condensable volatiles undergo secondary cracking, resulting in the formation of small molecules of non-condensable gases. The sugars, alcohols, ketones and acids in tar contain functional groups such as hydroxyl

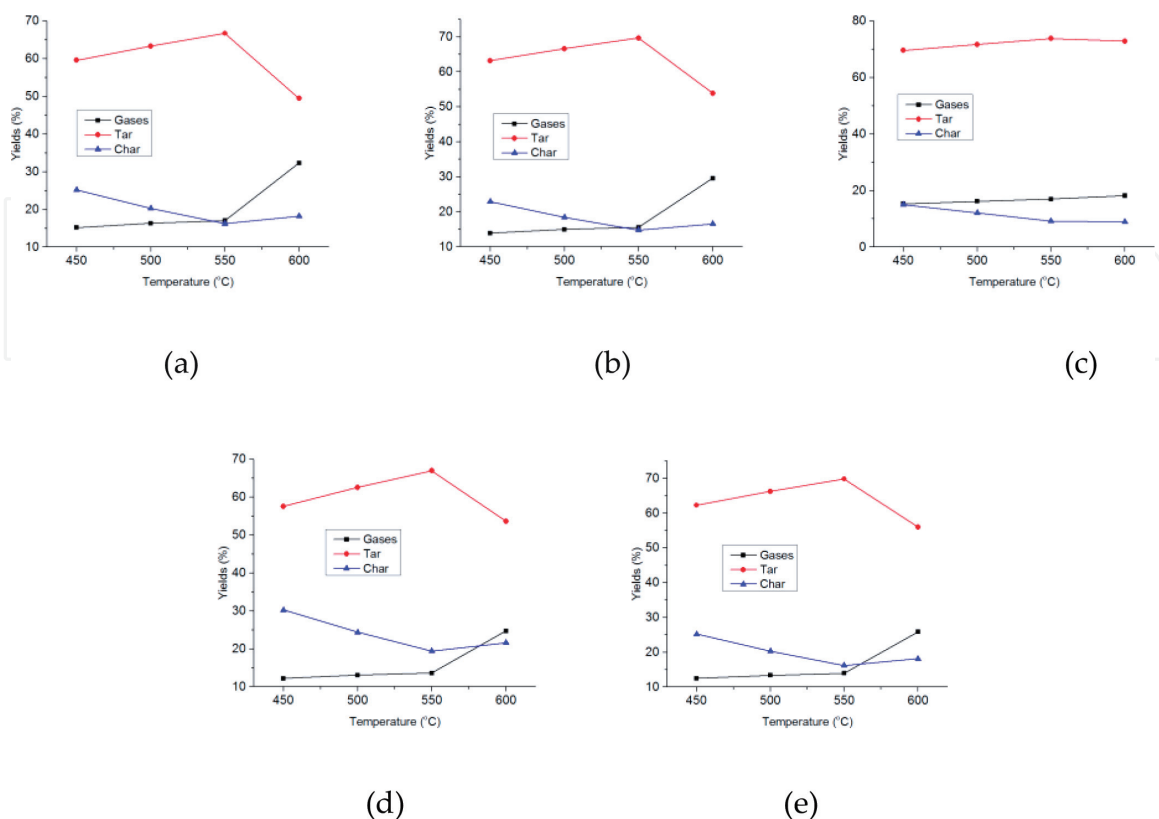


Figure 2. Yields of products from fast pyrolysis at different temperature of (a) Larch, (b) Poplar, (c) UF, (d) PBL, and (e) PBP.

and carboxyl groups, with the increase of temperature, these functional groups will decompose and produce gases such as CO and CO₂, resulting in the increase of gas phase products, which in turn reduced the yield of pyrolysis oil. During wood pyrolysis, lignin produces more fixed carbon than cellulose and hemicellulose, so the char yield of Larch and Poplar is higher than that of UF resin. Because the structure of UF resin is not complicated with wood, the yield change of UF resin in the pyrolysis process is not as obvious as that of wood and particle board, and the products are relatively few, mainly ester and amine substances [16].

Figures 3 and 4 show the cumulative histogram of the yield distribution from fast pyrolysis products of PBL and PBP and their components at different temperatures. From Figure 3, it can be seen that due to the effect of UF resin, the yield of fast

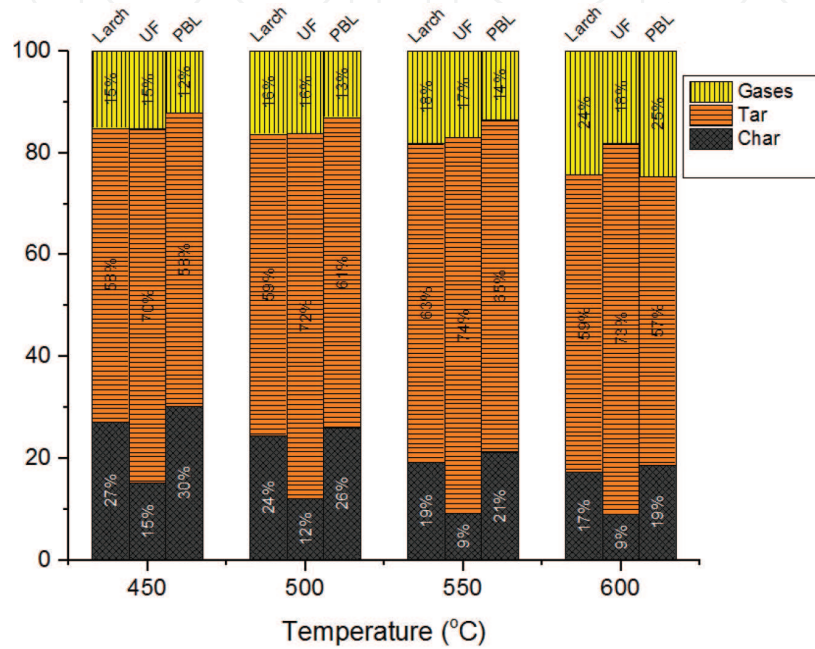


Figure 3. Distribution of products from fast pyrolysis of PBL at different temperatures.

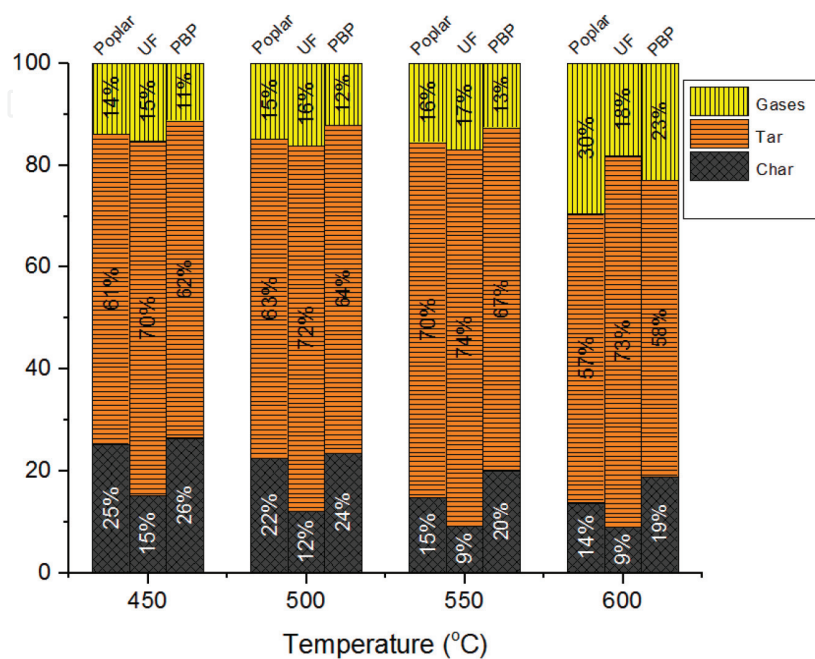


Figure 4. Distribution of products from fast pyrolysis of PBP at different temperatures.

pyrolysis carbon of PBL is higher than that of Larch, and it can be inferred that UF resin will prevent the pyrolysis of the particle board at high temperatures. As the temperature rises, this inhibition slows down, at 450°C, particle board fast pyrolysis carbon is 3% higher than Larch, while the pyrolytic carbon from particle board is only 1% higher than that from Larch when the temperature reaches 600°C. The yield of pyrolysis oil from fast pyrolysis of particle board is basically the same as the yield from Larch at 450°C, and the former is less than later when the temperature setting at 500 and 550°C. However, when the temperature exceeds 600°C, the yield of pyrolysis oil from fast pyrolysis of particle board is less than that from Larch. This is because the yield of pyrolysis oil of UF resin is high than that of wood, which resulted in the superposition effect; and on the other hand, it also shows that the introduction of UF resin has an impact on the yield of pyrolysis oil, which is more sensitive to temperature. From **Figure 4**, it can be seen that the effect of UF resin on the yield of fast pyrolysis products of PBP is similar to that of PBL, which has an inhibitory effect on the pyrolysis process of the particle board, and increases the yield of pyrolytic carbon of the particle board, along with the temperature increased this inhibition slows down.

Figure 5 shows the content comparison diagram of Tar and Char in the fast pyrolysis products from different materials. As can be seen from the figure, the Tar yield of the UF resin is significantly higher than that of other raw materials, and the Tar yield is higher at 550°C than at other temperatures. At 600°C, the decrease in Tar yield of other raw materials is more obvious with increasing temperature except UF resin. The Char yield of all raw materials decreased with the increase of temperature, but the Char yield of UF resin is significantly lower than other raw materials. The fast pyrolysis of wood and particle board yields of Tar and Char are basically the same, indicating that the addition of UF resin has little effect on the fast pyrolysis products Tar and Char.

3.1.2 Effect of carrier gas flow on yields of fast pyrolysis products

Figure 6 shows the yields of fast pyrolysis products of raw materials at different carrier gas flows. As can be seen from the figure, the increase in carrier gas flow rate can effectively prevent secondary cracking in the system, therefore, the yields of fast pyrolysis oil has been greatly improved with the increase of gas flow rate, and the production of pyrolytic carbon and gaseous has gradually decreased. When the flow rate of the carrier gas continues to increase, the secondary reaction has been at a relatively low level, and therefore, the effect on the product is relatively small. Compared with temperature, the influence of carrier gas flow rate on the distribution of fast pyrolysis products is relatively low, therefore, as long as gas phase residence time of less than 3 s can be ensured, a higher pyrolysis oil yield can be

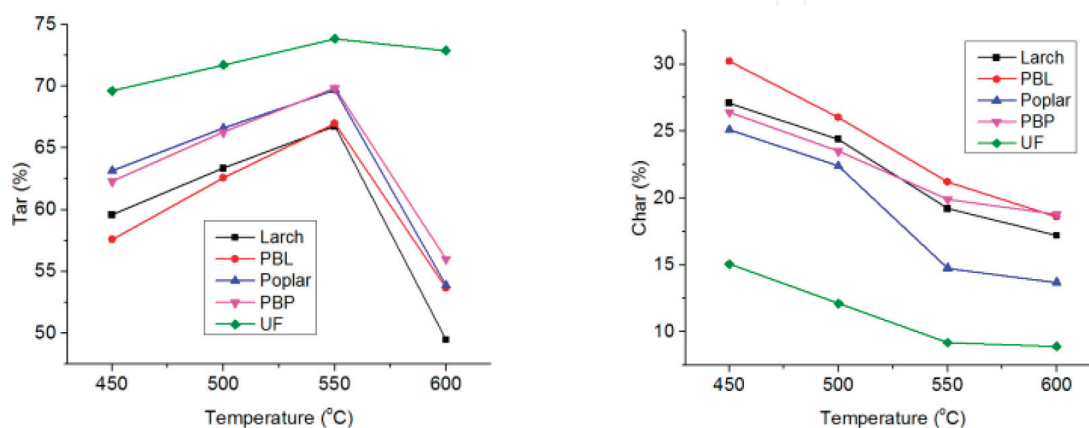


Figure 5.
Tar and char yields from fast pyrolysis of different raw materials at different temperatures.

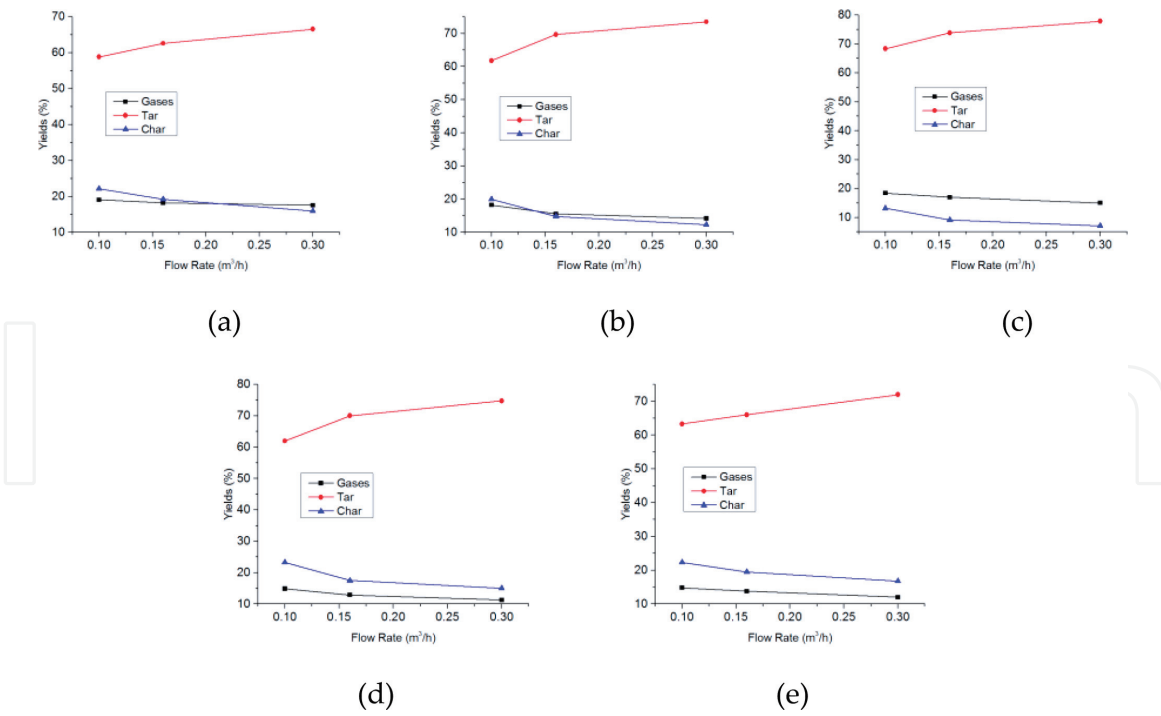


Figure 6. Yields of fast pyrolysis products at different carrier gas flow rate of (a) Larch, (b) Poplar, (c) UF, (d) PBL, and (e) PBP.

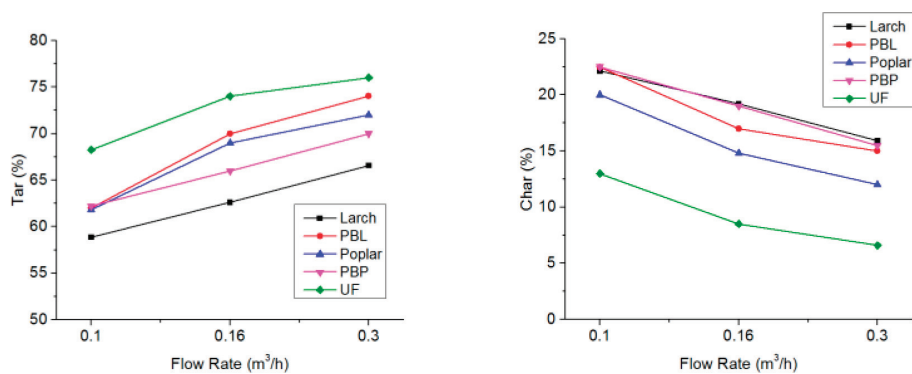


Figure 7. Tar and char yields from fast pyrolysis of different raw materials at different flow rates.

obtained. Of course, increasing the flow rate of the carrier gas will contribute to the increase of pyrolysis oil yield, where other conditions permit.

Figure 7 shows the comparison of Tar and Char contents in fast pyrolysis products of different raw materials. From the figure, we can see that the Tar yield of UF resin increases with the increase of the carrier gas flow rate, which is basically the same as other raw materials, indicating that the degree of secondary pyrolysis of UF resin is equivalent to that of other raw materials. It shows that under the condition of fast pyrolysis, the addition of UF resin has no obvious effect on the wood and particle board product.

3.2 Influence of pyrolysis conditions on composition of fast pyrolysis products of waste particle board

3.2.1 Influence of pyrolysis conditions on distribution of gas product composition

Figure 8 changes of the gas composition in fast pyrolysis of raw materials at different temperatures. As can be seen from the figure, at different temperatures,

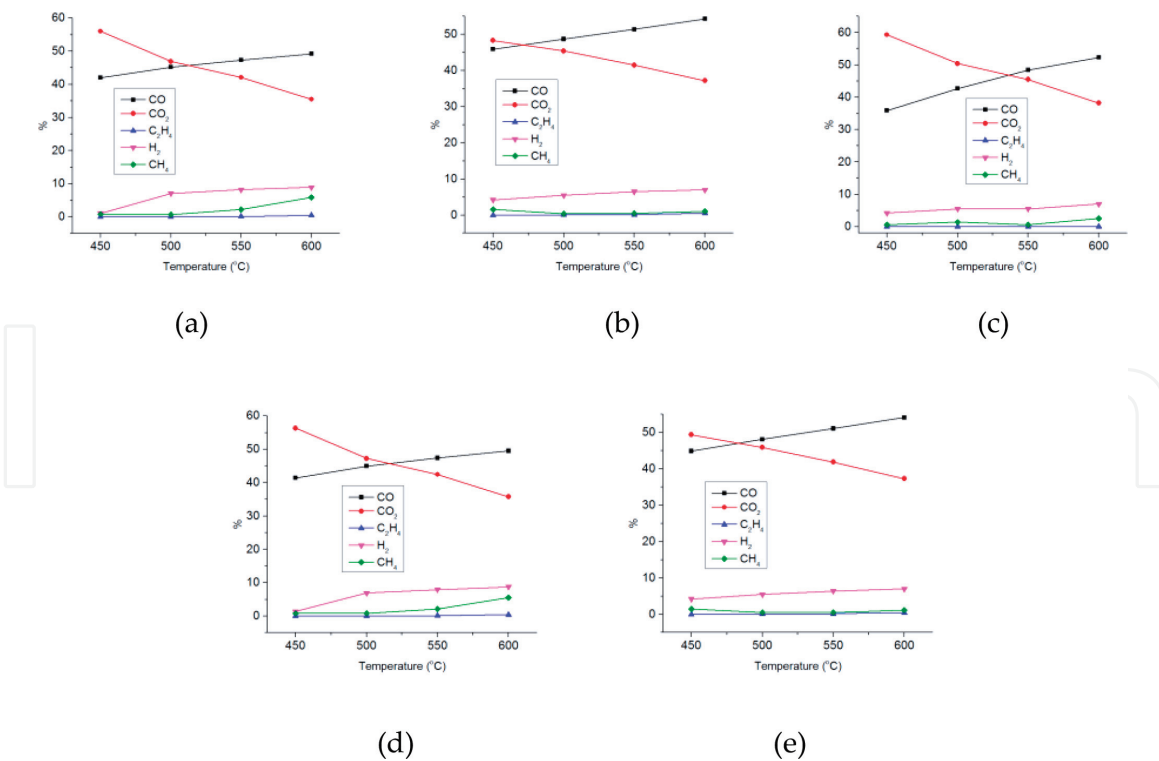


Figure 8.
 Gaseous products distribution from fast pyrolysis at different temperature of (a) Larch, (b) Poplar, (c) UF, (d) PBL, and (e) PBP.

the fast pyrolysis gases of various raw materials are mainly CO and CO₂. With the increase of temperature, the CO content increased while the CO₂ content decreased, crossover occurred within the experimental temperature range, the temperature at this intersection varies depending on the composition of the raw materials. This aspect shows that the competitive reaction of the gas generated during the fast pyrolysis process is beneficial to the production of CO₂ at low temperatures, and is more conducive to the production of CO at high temperatures. It shows that the CO and CO₂ generation mode and mechanism are different during the fast pyrolysis process, and the effect of temperature on them is opposite. On the other hand, the cracking of the raw material in the fast pyrolysis process is accompanied by the secondary cracking of the primary volatiles, which means that the secondary cracking of the volatiles will generate more CO at high temperature, but it will not contribute much to the generation of CO₂, analysis shows that the CO is mainly produced by the cleavage of organic acids and aldehydes containing carbonyl groups and carboxyl groups. In addition, CO₂ reacts with the pyrolytic carbon in the reaction system to convert to CO at higher temperatures. The experimental results are similar to the fast pyrolysis experiments performed on different biomass in the literature.

As can be seen from **Figure 8**, the yield of several other gases is very small, with a relatively high H₂ content of about 5–10%, while the amount of CH₄ and C₂H₄ is less than 2%. With the increase of temperature, the amount of these gases has increased to some extent, and the overall calorific value of the fast pyrolysis gas has increased. The main reasons for the increase of H₂ yield are: the condensation of char; secondary reaction of tar, such as the polycondensation of aldehyde and ketone compounds; cracking of alkanes and alkenes. With the increase of temperature, the polycondensation reaction is enhanced. Some compounds in tar undergo polycondensation reaction to form benzene ring and other structures, and form H·, which eventually leads to the increase of H₂ content. For hydrocarbons, the C-H bond and the stability of C-C bond in the order: C≡C > C=C > C-H > C-C, however,

at high temperatures alkane content in tar is less, and alkenes, alkynes and aromatic compounds content is higher, compared with the C-H, C-C bond in tar is less, resulting in high temperature tar cracking process of CH_4 is less than the H_2 . The variation pattern of CH_4 and C_2H_4 is similar to that of CO . In the study of biomass thermal cracking, the generation of CH_4 is mostly derived from the methoxy group in lignin structure, and the secondary decomposition of the volatile component of cellulose polymer can also produce CH_4 . The detected unsaturated hydrocarbons are mainly C_2H_4 , the yield of C_2H_4 is similar to that of CH_4 , and the content in the gas is also very low. The analysis of its formation may be obtained from the thermal decomposition of unsaturated fatty acids.

Figure 9 shows the comparison of CO and CO_2 contents in fast pyrolysis gases of different raw materials. From the figure, we can see that the CO yield of UF with temperature rise is more obvious than that of wood and particle board, but the trend of CO_2 falling with temperature is basically the same. It shows that the UF contains a large amount of carbonyl groups which will be pyrolyzed to generate more CO during the fast pyrolysis process. Compared with two types of wood, the amount of CO and CO_2 produced from Larch is higher than that produced from Poplar, this is caused by the difference in the composition of the two types of wood. The yields of CO and CO_2 produced by pyrolysis of wood and particle board are basically the same, indicating that the addition of UF resin has no obvious effect on the fast pyrolysis of gas products.

Figure 10 is the variation diagram of the components of gaseous products from fast pyrolysis at different carrier gas flow rates. From this figure, it can be seen that under different carrier gas flow rates, CO and CO_2 are predominant in the fast pyrolysis gas composition of various raw materials. With the increase of flow rate, the content of CO and other gases have decreased to varying degrees, while the CO_2 content has increased. An increase in the flow rate of the carrier gas leads to a reduction in the retention time of the gas phase, thereby reducing the secondary cracking of the primary volatiles, so that the overall production of the gas product will decrease. The decrease of CO content and the increase of CO_2 content indicate that the secondary cracking of volatiles is more likely to produce CO , but has little effect on CO_2 . Therefore, the percentage of CO_2 will increase as the total amount of gas decreases.

Figure 11 shows the comparison of CO and CO_2 contents in fast pyrolysis gases of different raw materials. From the figure, we can see that the CO yield of UF resin decreases with the increase of the carrier gas flow rate, which is basically the same as other raw materials, indicating that the degree of secondary pyrolysis of UF resin is equivalent to that of other raw materials. It shows that under the condition of fast pyrolysis, the addition of UF resin has no obvious effect on the wood gas product.

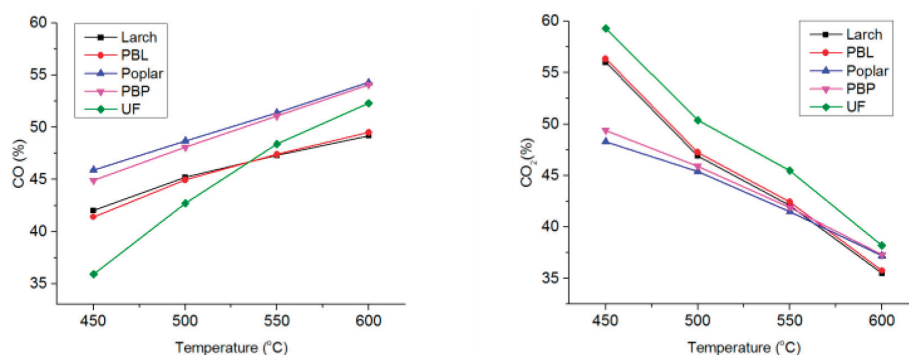


Figure 9.
CO and CO_2 yields from fast pyrolysis of different raw materials at different temperatures.

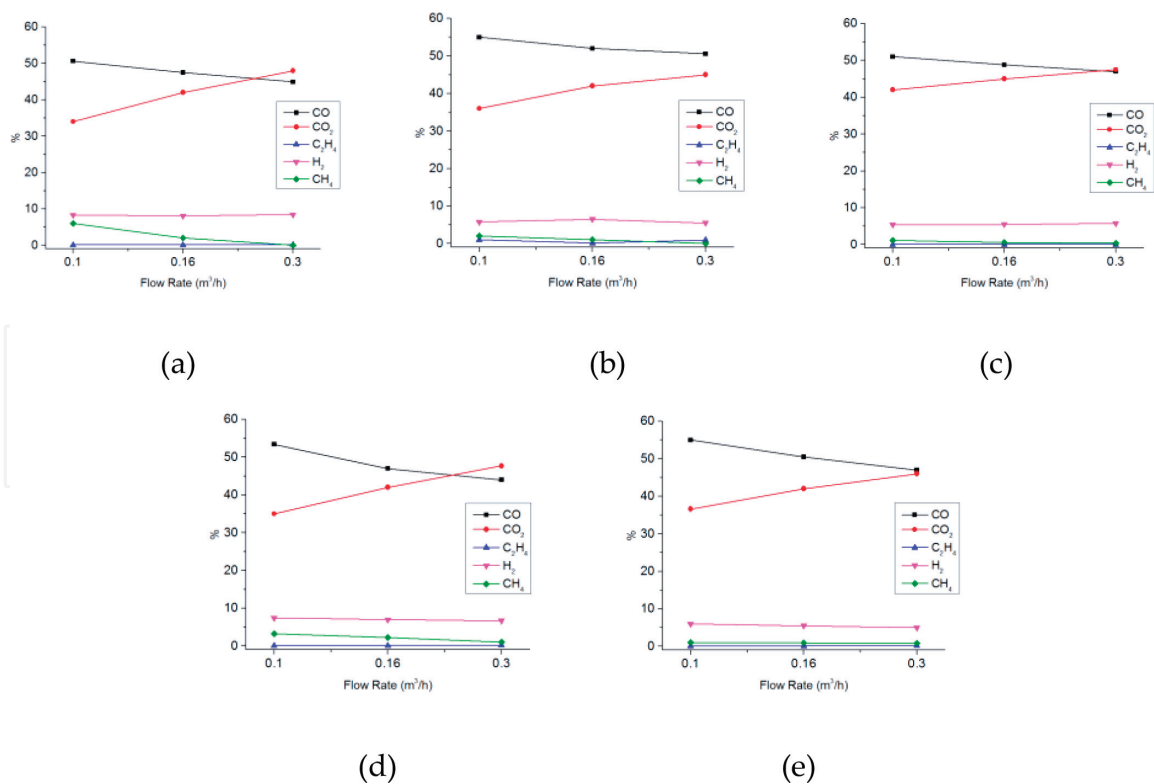


Figure 10. Gaseous products distribution from fast pyrolysis at different carrier gas flow rates of raw materials: (a) Larch, (b) Poplar, (c) UF, (d) PBL, and (e) PBP.

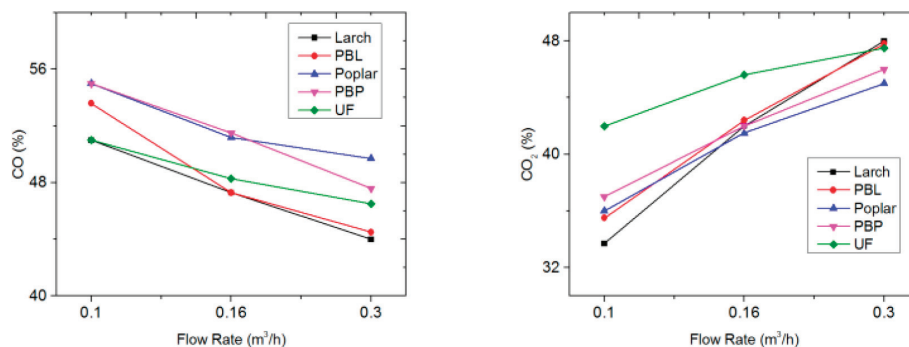


Figure 11. CO and CO₂ contents fast pyrolysis products at different carrier gas flow rates.

3.2.2 Influence of pyrolysis conditions on the distribution of liquid product components

Figure 12 is a GC/MS total ion chromatogram (TIC) of the liquid product from fast pyrolysis of Larch, UF, and PBL, at 500°C. Due to the relatively simple structure of the UF resin, the TIC peak of the products from fast pyrolysis of UF resin is significantly lower than the TIC peak of the products from pyrolysis of wood and particle board, and no product peak appears after more than 30 minutes of retention time. When using the NIST library search, about 90 substances can be detected for the pyrolysis liquid phase products of particle board and wood raw materials under different conditions. The UF resin produced the most substances when it was pyrolyzed at 500°C, and only 37 products were found. The main components and relative content of liquid phase products of Larch, UF resin and PBL are shown in the appendix table. The spectral peaks of the PBL are very similar to those of the Larch, indicating that the main components of the pyrolysis products of the waste particle board are the same as the Larch.

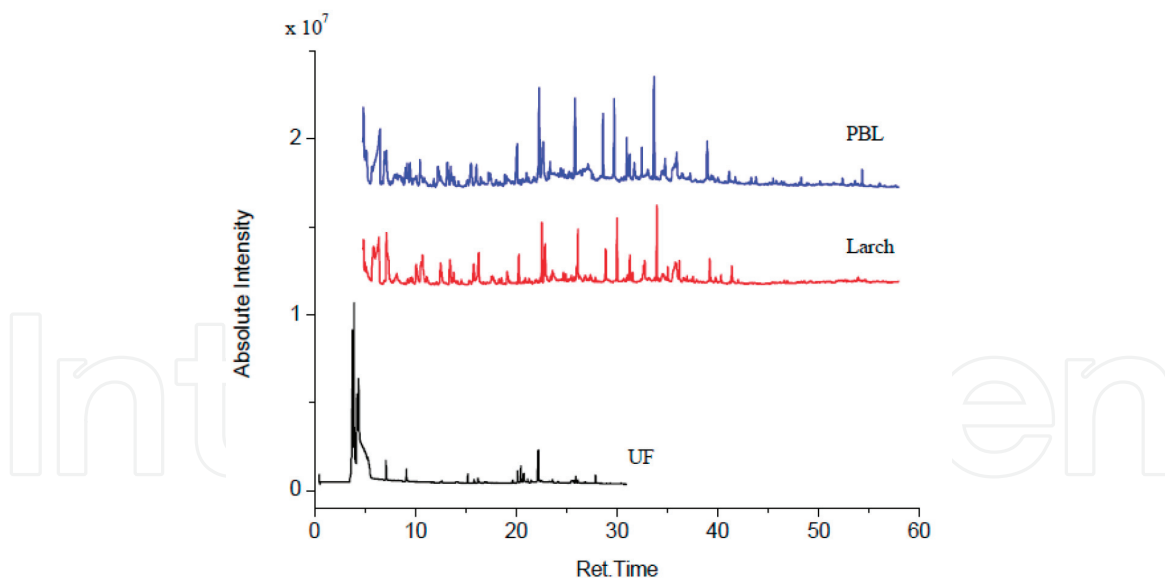


Figure 12.
TIC spectra of liquid products from fast pyrolysis of Larch, UF and PBL.

By classifying and comparing the pyrolysis liquid product components, the effect of pyrolysis conditions on the main categories of fast pyrolysis products can be analyzed. The products detected by GC/MS are classified into 13 categories, which are amines, alcohols, phenols, aldehydes, acids, ketones, esters, ethers, sugars, hydrocarbons, heterocyclic-N, other-N and others. From the appendix table, it can be seen that nitrogenous substances are the main components of UF resin pyrolysis liquid. UF resin contains amino, carbonyl, methylene and other groups, during the pyrolysis of UF resin, a group of hydroxyl methyl groups first split into formaldehyde and then produce nitrogen-containing volatile components with C-N bond breaking. The relative content of methyl isocyanate reaches up to 39.25%, in addition, other nitrogenous substances, such as ethyleneimine (13.68%), ethyl pyruvate (10.67%), 2,3-diazabicyclo [2.2.1]-hept-2-ene decanols (5.13%), l-alanine ethylamide, (S)-(3.91%), can also be detected in the pyrolysis liquid of UF resin. Compared with the composition of UF resin, the pyrolytic liquid products of Larch and PBL are very complicated. The products of wood mainly include alcohols, ketones, aldehydes, ketone derivatives and carbohydrates. The major constituent is hydroxyacetone and the relative content is 7.43%, other ketone derivatives, such as 1,3-cyclopentadione (3.12%) and 2,3-glutaric ketone (2.53%) can also be detected in the pyrolysis liquid of Larch, these ketone derivatives are generated by the pyrolysis of holocellulose. Lignin structure is rich in methoxy, and most phenolic compounds in the pyrolysis solution have the methoxyl chain. During the pyrolysis, the lignin molecular chain is cracked and the fragments are rearranged. The relative content of cis-isoeugenol and 2-methoxyl-4-vinyl phenol in Larch liquid phase products can reach 4.96 and 3.08%, respectively. In addition, phenolic compounds such as 4-ethyl guaiacol (1.38%), guaiacol (2.76%), 4-methyl guaiacol (2.53%), eugenol (1.32%) and phenol (0.33%) can also be detected. Particle board pyrolysis liquid product variety is one of the most in the three kinds of raw materials, main components of acetic acid (13.04%), (E)-iso-eugenol (5.22%), guaiacol (5.07%), cyclopropylmethyl alcohol (4.81%), 4-methyl hydroxyacetone (4.24%), guaiacol (3.97%), 4-hydroxy-3-methyl acetophenone (3.48%), 3-methyl-1, 2-ring glutaric ketone (2.98%) and furfuryl alcohol (2.75%), and other substances phenols, alcohols and ketones. Compared with Larch pyrolysis liquid phase, more Larch and

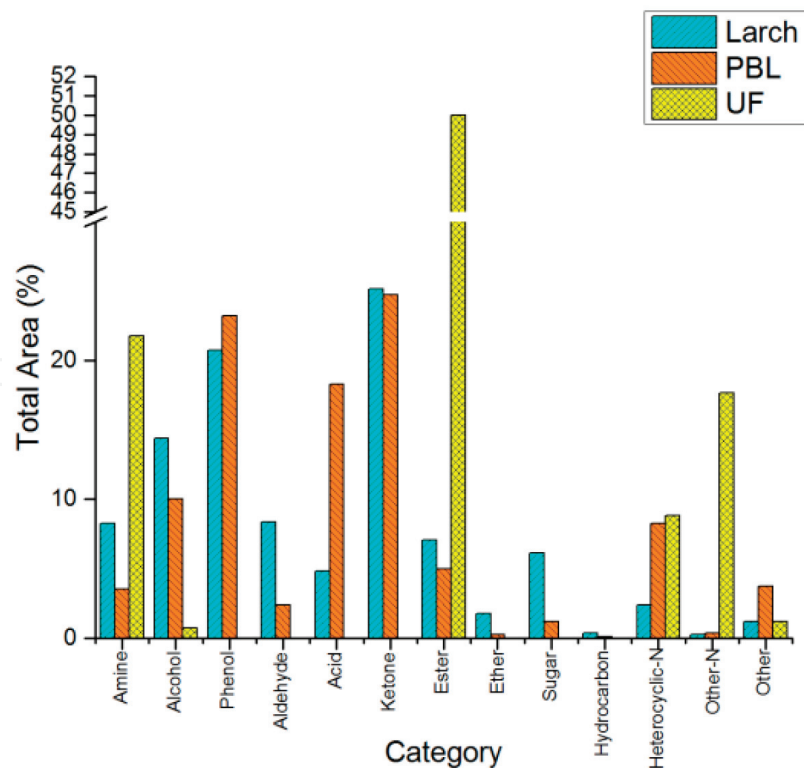


Figure 13.
Subtotal amount of different categories of fast pyrolysis liquid products ($T = 500^{\circ}\text{C}$).

UF resin synergistic reaction products, such as 1,3,4-trimethyl-1,7-dihydro-6h-pyrazole and [3,4-b] pyridine 6-ketone, were obtained in the pyrolysis liquid phase products of particle board [16].

Figure 13 is a summary of the main components of the fast pyrolysis liquid of Larch, UF and PBL at 500°C . As can be seen from the figure, the type of fast pyrolysis liquid product of PBL is the same as that of Larch, and is mainly based on alcohol, phenol, acid, and ketone, the maximum content of esters in the urea-formaldehyde resin pyrolysis liquid phase product is nearly 50%, which together with amines, nitrogen heterocycles and other nitrogen-containing compounds form the main liquid phase products. Due to the effect of UF resin, the product of PBL has a greater change than Larch, and the nitrogen heterocyclic compound in the PBL has been greatly improved compared to wood. In addition, acid and phenolic substances have also been improved to varying degrees, while amines, alcohols, aldehydes, esters, sugars and other components have been reduced to varying degrees. The change of these components is due to the fact that the introduced UF resin itself is produced during the fast pyrolysis process, for example, the nitrogen heterocyclic compounds are mainly formed by the cyclization of the amide nitrogen from fast pyrolysis of UF resin. However, more compositional changes should result from the complex chemical reactions that occurred between the UF resin and wood components during the fast pyrolysis process, for example, amines and esters are the main products of UF resin, but the content of PBL products is lower than that of wood products. Phenolics and acids were not detected in the UF resin pyrolysis liquid phase product, but the content of PBL products was higher than that of wood. Therefore, during the fast pyrolysis of the particle board, a strong interaction occurs between the wood components and the UF resin component, in other words, chemical reactions occurred between the derivatives from UF resin and wood during fast pyrolysis.

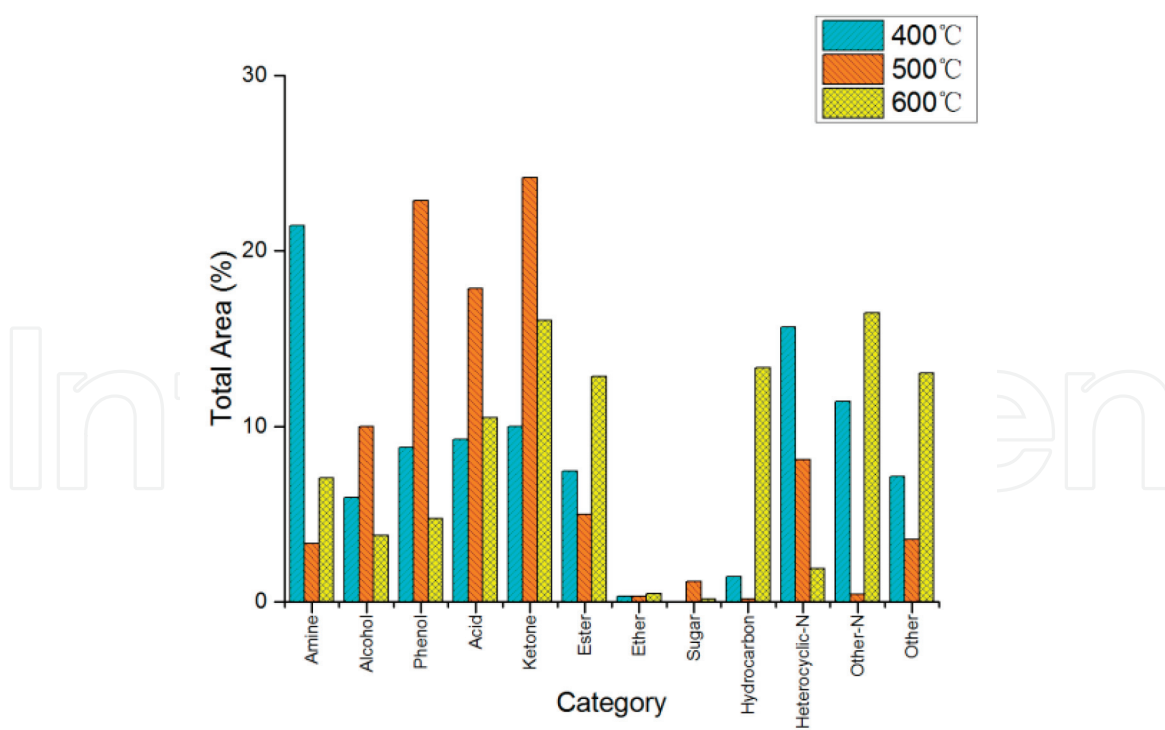


Figure 14. Subtotal amounts of different categories of liquid products from fast pyrolysis of PBL at different temperatures.

Temperature is one of the main factors affecting fast pyrolysis. **Figure 14** is a summary of the main components of liquid products from fast pyrolysis of PBL at different temperatures. From the figure, it can be seen that the content of liquid products from fast pyrolysis of the PBL at 500°C is generally higher than that at 400 and 600°C, such as alcohol, phenol, acid, ketone, etc., this is consistent with the trend of maximum yield of pyrolysis oil obtained at a fixed bed fast pyrolysis experiment at 500°C. When the temperature is lower, the cracking of raw materials is incomplete and the yield of volatiles is low, when the temperature is higher, more secondary cracking occurs in the volatiles and they are converted into small molecules. The effect of temperature on the specific components of the product and its mechanism remain to be further studied.

It can also be seen from **Figure 14** that the nitrogen-containing compounds account for the most part in liquid phase products from fast pyrolysis of particle board at a lower temperature of 400°C, mainly amines, nitrogen heterocyclic, etc., indicating that at low temperatures UF resin already be decomposed to produce liquid products. When the temperature rises to 500°C, the amines, nitrogen heterocycles and other liquid nitrogen compounds in the product have been significantly reduced, indicating that some low-stability substances undergo secondary cracking to generate small-molecule gas-phase compounds, while the secondary cleavage of nitrogen heterocycles with higher stability is still not obvious. When the temperature continues to increase to 600°C, the nitrogen heterocyclic ring in the product is significantly reduced, indicating that at higher temperatures, a large number of nitrogen heterocycles also undergo cracking reactions. As a result, amines, nitrogen-containing esters, and other nitrogen-containing compounds are produced, making the amount of these substances significantly higher than at 500°C. These changes are similar to the effects of temperature on pyrolysis yields. Therefore, in the fast pyrolysis process, the temperature has a decisive effect on the product yield and composition.

Figure 15 is a summary of the main components of the liquid phase product of the PBL at different carrier gas flow rates. The flow rates were set to 100, 50 and

10 ml/min. It can be seen from the figure that with the decrease of the carrier gas flow rates, the gas phase residence time is prolonged and the secondary cracking of the volatiles is enhanced, more small molecules are produced. From the liquid product search results, it was found that the product types did not change, the content of the higher molecular weight material decreased, and the content of the

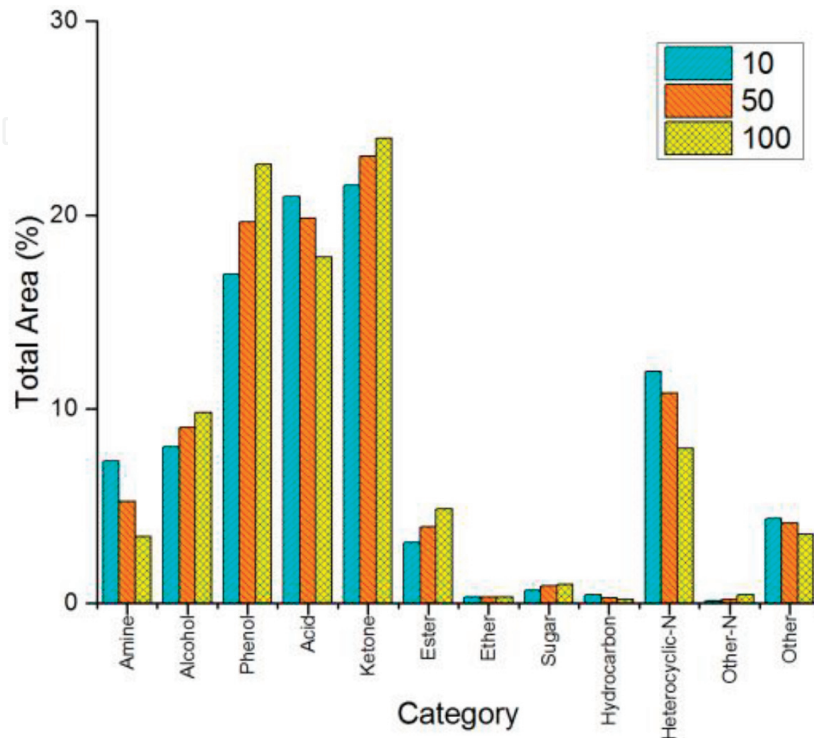


Figure 15. Subtotal amounts of different categories of PBL fast pyrolysis liquid products at different carry gas flow rates.

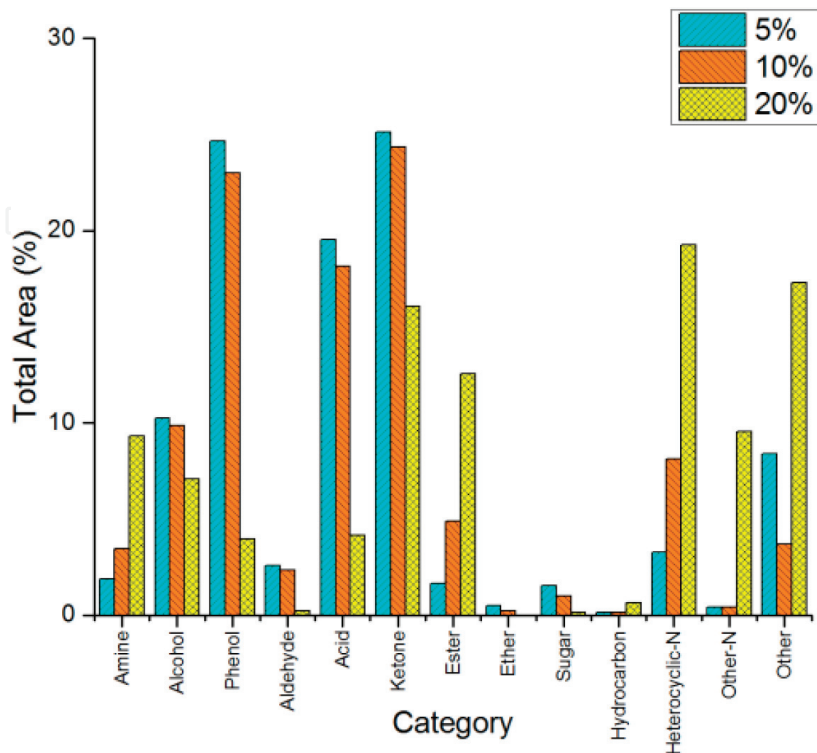


Figure 16. Subtotal amounts of different categories liquid products from fast pyrolysis of PBL with different adhesive amounts.

lower molecular weight material increased. Under different temperature conditions, the yield of the same product is not much different, which indicates that the carrier gas flow rates has little influence on the product quantity, and the overall influence degree is not as obvious as the temperature.

Figure 16 is a summary of the main components of the liquid phase products from fast pyrolysis of PBL with different adhesive amount.

As can be seen from **Figure 16**, the increase in adhesive amount directly results in an increase in all nitrogenous products in the product, including amines, nitrogen heterocycles, and other nitrogen-containing compounds. In addition, the amount of ester products has also been significantly increased, the reason is that many esters contain nitrogen, which means that the amide nitrogen in the raw material is involved in a large number of esterification reactions. When the amount of adhesive is at a little level, UF resin has a promoting effect on the formation of phenol in wood, and plays a similar catalyst effect; when the amount of adhesive increases, the phenolics in the particle board begin to drop; when the amount of adhesive is 20%, it even drops to 4%, which is less than a quarter of the phenol content (20.5%) in fast pyrolysis products of wood. It is speculated that in a fast pyrolysis system, too much UF resin will compete with the phenol-forming reaction, generating more amine and nitrogen heterocyclic structures. In comparison, the effects of UF resin on acid substances are similar to those on phenolic substances, less adhesive amounts contribute to the formation of acids, while an increase in the amount of sizing inhibits acid production and appears to decrease.

4. Conclusions

Fast pyrolysis experiments of Larch and Poplar, UF, PBL and PBP were carried out, and the yields of pyrolysis products and its composition were analyzed. The results show that when the pyrolysis temperature is between 400 and 600°C, the gas yield steadily increase as the temperature increases, and the pyrolysis carbon yield continues to decrease, while the yield of pyrolysis oil increased at first and then decreased afterwards, and reached a maximum at 550°C. The carbon yield from fast pyrolysis of particle board is higher than that of wood, indicating that UF resin will prevent particle board decomposing, and this impact goes weak with increasing of temperature.

Compared with temperature, the influence of the carrier gas flow rates on the yields of products and its distribution is relatively low. Increasing of carrier gas flow rate can effectively prevent the occurrence of secondary cracking in the system and increase the pyrolysis oil yield. The gas products from fast pyrolysis of waste particle board are mainly CO and CO₂, as well as relatively small amounts of CH₄, C₂H₄, H₂, etc. With the increase of temperature, the content of CO₂ decreased and the contents of other gases increased. Among them, the tendency of CO obviously rose, and the calorific value of gas has increased. Under the conditions of fast pyrolysis, the effect of UF resin on the gas composition of particle board is not obvious.

Compared with wood, the main components of pyrolysis liquid phase products of waste particle board have not changed much, while the nitrogenous substances such as amines and nitrogen heterocycles are mainly increased, which promoted the formation of phenols and acids and prevented the formation of aldehydes, sugars, and alcohols. The temperature has little effect on the product type, but has a great influence on the yields. The carrier gas flow rate has little effect on the product composition. The effect of adhesive amount on the composition of the product is unclear.

Acknowledgements

The work was supported by the Fundamental Research Funds for the Central Universities (2017ZY32).

A. Main compounds of fast pyrolysis liquid products of Larch, UF and PBL

No.	Name	Molecular formula	Molecular weight	Larch	Area % PBL	UF
1	Ethyleneimine	C ₂ H ₅ N	43	\	\	13.68
2	Formamide	CH ₃ NO	45	0.27	1.61	0.11
3	Aminoacetonitrile	C ₂ H ₄ N ₂	56	\	\	0.03
4	Methyl isocyanate	C ₂ H ₃ NO	57	\	1.23	39.25
5	Acetamide	C ₂ H ₅ NO	59	6.53	0.57	\
6	N-Methylformamide	C ₂ H ₅ NO	59	\	0.64	\
7	Trimethylamine	C ₃ H ₉ N	59	\	\	2.56
8	Acetic acid	C ₂ H ₄ O ₂	60	2.25	13.04	\
9	Ethylene glycol	C ₂ H ₆ O ₂	62	\	0.68	\
10	Pyrrrole	C ₄ H ₅ N	67	0.42	1.83	\
11	Allyl cyanide	C ₄ H ₅ N	67	\	\	0.05
12	2,5-Dihydrofuran	C ₄ H ₆ O	70	0.3	0.13	\
13	Cyclopropylmethanol	C ₄ H ₈ O	72	3.34	4.81	\
14	N-Methylacetamide	C ₃ H ₇ NO	73	\	0.52	\
15	Hydroxyacetone	C ₃ H ₆ O ₂	74	7.43	4.24	\
16	Methyl acetate	C ₃ H ₆ O ₂	74	\	1.41	\
17	Methylurea	C ₂ H ₆ N ₂ O	74	\	\	0.09
18	Methyl carbamate	C ₂ H ₅ NO ₂	75	\	\	0.14
19	Pyridine	C ₅ H ₅ N	79	0.14	\	\
20	Pyrimidine	C ₄ H ₄ N ₂	80	\	0.47	\
21	N-methylpyrrole	C ₅ H ₇ N	81	0.32	1.39	\
22	3-Methylpyrrole	C ₅ H ₇ N	81	\	0.33	\
23	1,3,5-Triazine	C ₃ H ₃ N ₃	81	\	\	1.21
24	1,4-Pentadien-3-one	C ₅ H ₆ O	82	0.39	\	\
25	N-methylimidazole	C ₄ H ₆ N ₂	82	\	0.56	0.06
26	2(5H)-Furanone	C ₄ H ₄ O ₂	84	1.92	2.19	\
27	N,N-Dimethylaminoacetonitrile	C ₄ H ₈ N ₂	84	\	1.12	0.66
28	Succinaldehyde	C ₄ H ₆ O ₂	86	2.01	\	\
29	2,3-Butanedione	C ₄ H ₆ O ₂	86	\	1.05	\
30	Beta-butyrolactone	C ₄ H ₆ O ₂	86	\	\	0.21
31	1-Hydroxy-2-butanone	C ₄ H ₈ O ₂	88	\	0.98	\
32	N,N-Dimethylurea	C ₃ H ₈ N ₂ O	88	\	\	0.56

No.	Name	Molecular formula	Molecular weight	Larch	Area % PBL	UF
33	Carbohydrazide	CH ₆ N ₄ O	90	\	\	0.2
34	Methyl hydroxyacetate	C ₃ H ₆ O ₃	90	0.51	0.47	\
35	Phenol	C ₆ H ₆ O	94	0.33	\	\
36	3-Methylpyridazine	C ₅ H ₆ N ₂	94	0.17	\	\
37	N-Vinylimidazole	C ₅ H ₆ N ₂	94	\	\	0.1
38	2,3-Dimethyl-1H-pyrrole	C ₆ H ₉ N	95	0.25	\	\
39	3-Hydroxypyridine	C ₅ H ₅ NO	95	0.56	\	\
40	2,5-Lutidine	C ₆ H ₉ N	95	\	0.57	\
41	Furfural	C ₅ H ₄ O ₂	96	2.21	1.34	\
42	4-Imidazole formaldehyde	C ₄ H ₄ N ₂ O	96	0.16	\	\
43	4-Cyclopentene-1,3-dione	C ₅ H ₄ O ₂	96	0.29	0.22	\
44	3-Methyl-2-cycloalkenone	C ₆ H ₈ O	96	\	0.3	\
45	2,5-Dimethylfuran	C ₆ H ₈ O	96	\	1.24	\
46	2-Amino-1,3,5-triazine	C ₃ H ₄ N ₄	96	\	\	0.27
47	2,3-Diazabicyclo[2.2.1]-hept-2-ene decanols	C ₅ H ₈ N ₂	96	\	\	5.13
48	Furfuryl alcohol	C ₅ H ₆ O ₂	98	2.55	2.75	\
49	1,3-Cyclopentadione	C ₅ H ₆ O ₂	98	3.12	\	\
50	1,2-Cyclopentadione	C ₅ H ₆ O ₂	98	\	1.51	\
51	2-Ethylene-3-vinyl epoxy-ethane	C ₆ H ₁₀ O	98	0.41	\	\
52	Ethyl cyanofornate	C ₄ H ₅ NO ₂	99	\	0.21	\
53	3-Amino-5-hydroxypyrazole	C ₃ H ₅ N ₃ O	99	\	0.22	\
54	2-Methyl-2-pentene-1-alcohol	C ₆ H ₁₂ O	100	0.5	\	\
55	2,3-Glutaric ketone	C ₅ H ₈ O ₂	100	2.53	0.27	\
56	2-Methyl-3-pentone	C ₆ H ₁₂ O	100	0.29	0.54	\
57	Tetrahydro-2H-pyran-3-ketone	C ₅ H ₈ O ₂	100	0.47	0.52	\
58	Succinic anhydride	C ₄ H ₄ O ₃	100	\	\	0.05
59	2, 2-Dimethyl-1-butanol	C ₆ H ₁₄ O	102	\	0.37	\
60	Methyl pyruvate	C ₄ H ₆ O ₃	102	2.68	\	\
61	Acetic anhydride	C ₄ H ₆ O ₃	102	0.78	\	\
62	M-Cresol	C ₇ H ₈ O	108	0.22	0.21	\
63	2-Acetylpyrrole	C ₆ H ₇ NO	109	0.18	0.25	\
64	2, 3-Diaminopyridine	C ₅ H ₇ N ₃	109	\	\	0.24
65	2H-Tetrazole-2-ethyl acetonitrile	C ₃ H ₃ N ₅	109	\	0.41	\
66	5-Methylfurfural	C ₆ H ₆ O ₂	110	0.61	0.86	\
67	2,3-Dimethyl-2-cyclopentene-1-ketone	C ₇ H ₁₀ O	110	\	0.16	\
68	2-Acetylfuran	C ₆ H ₆ O ₂	110	\	0.19	\
69	2-Amino-3-hydroxypyridine	C ₅ H ₆ N ₂ O	110	\	\	0.07
70	Isocytosine	C ₄ H ₅ N ₃ O	111	0.23	\	\
71	3-Hydroxypyridine-N-oxide	C ₅ H ₅ NO ₂	111	\	\	0.39
72	N-Ethylidene-1-pyrrolidine	C ₆ H ₁₂ N ₂	112	\	\	0.83

No.	Name	Molecular formula	Molecular weight	Larch	Area % PBL	UF
73	3-Methyl-1,2-cyclopentanedione	C ₆ H ₈ O ₂	112	1.72	2.98	\
74	3-Methyl-1,2-cyclopentanedione	C ₆ H ₈ O ₂	112	1.2	\	\
75	Cyclopentyl ethanone	C ₇ H ₁₂ O	112	\	0.14	\
76	3-Isopropoxypropionitrile	C ₆ H ₁₁ NO	113	\	0.11	\
77	2,3-Dimethylene-1,4-butanediol	C ₆ H ₁₀ O ₂	114	\	0.51	\
78	Trans-2-hexenoic acid	C ₆ H ₁₀ O ₂	114	0.28	\	\
79	2,5-Dione piperazine	C ₄ H ₆ N ₂ O ₂	114	\	\	0.25
80	5,6-Dihydrouracil	C ₄ H ₆ N ₂ O ₂	114	\	\	0.09
81	2,6-Dimethylpiperazine	C ₆ H ₁₄ N ₂	114	\	\	0.56
82	l-Alanine ethylamide, (S)-	C ₅ H ₁₂ N ₂ O	116	\	\	3.91
83	Acetylacetone peroxide	C ₅ H ₈ O ₃	116	0.68	1.02	\
84	Ethyl pyruvate	C ₅ H ₈ O ₃	116	\	\	10.67
85	1,4-Dioxane-2,5-diol	C ₄ H ₈ O ₄	120	5.66	\	\
86	1-Methyl-2-pyrroloethane cyanide	C ₇ H ₈ N ₂	120	\	\	0.11
87	(Ethyleneoxy)benzene	C ₈ H ₈ O	120	0.34	\	\
88	Guaiacol	C ₇ H ₈ O ₂	124	2.76	5.07	\
89	N-(S-triazolyl)acetamide	C ₄ H ₆ N ₄ O	126	\	0.08	\
90	2-Methyl-1,5-heptadiene-4-alcohol	C ₈ H ₁₄ O	126	0.14	\	\
91	Maltol	C ₆ H ₆ O ₃	126	0.34	0.36	\
92	5-Hydroxymethylfurfural	C ₆ H ₆ O ₃	126	0.67	\	\
93	Imidazol-4-acetic acid	C ₅ H ₆ N ₂ O ₂	126	\	2.65	\
94	3-Ethyl-4-methyl-3-pentene-2-ketone	C ₈ H ₁₄ O	126	0.39	\	\
95	2-Methyl cycloheptanone	C ₈ H ₁₄ O	126	0.6	\	\
96	Ethyl cyclopentenolone	C ₇ H ₁₀ O ₂	126	\	0.53	\
97	1-Methyluracil	C ₅ H ₆ N ₂ O ₂	126	\	0.12	\
98	2-(1,1-Dimethylethyl)-1,3-dimethylnitrogen propidine	C ₈ H ₁₇ N	127	\	\	1.46
99	2,3-Dimethylcyclohexanol	C ₈ H ₁₆ O	128	0.26	\	\
100	1-Cyclopropyl-1-pentyl alcohol	C ₈ H ₁₆ O	128	\	0.17	\
101	6-Heptanoic acid	C ₇ H ₁₂ O ₂	128	0.38	\	\
102	3-Symplectic ketone	C ₈ H ₁₆ O	128	\	0.43	\
103	1-Methyl-hydrouracil	C ₅ H ₈ N ₂ O ₂	128	\	1.53	0.35
104	1,3,5-Trimethyl-hexamethyl-1,3,5-triazine	C ₆ H ₁₅ N ₃	129	\	\	3.16
105	L-Ornithine	C ₅ H ₁₂ N ₂ O ₂	132	\	\	0.1
106	4-Methyl guaiacol	C ₈ H ₁₀ O ₂	138	2.53	3.97	\
107	Hexamethylenetetramine	C ₆ H ₁₂ N ₄	140	\	\	0.03
108	3-Oxy-1-cyclopentene-1-acetate	C ₇ H ₈ O ₃	140	0.63	\	\
109	Dipropylene aminoacetonitrile	C ₈ H ₁₆ N ₂	140	\	\	0.14
110	Heptyl isocyanate	C ₈ H ₁₅ NO	141	0.43	\	\
111	(1Z)-2-Ethylcyclohexanone oxime	C ₈ H ₁₅ NO	141	0.28	\	\
112	4-Octyne-3,6-diol	C ₈ H ₁₄ O ₂	142	0.27	\	\

No.	Name	Molecular formula	Molecular weight	Larch	Area % PBL	UF
113	Nonyl aldehyde	C ₉ H ₁₈ O	142	1.02	\	\
114	4-Ethyl-2,2-dimethylhexane	C ₁₀ H ₂₂	142	0.32	\	\
115	4-Amino-N-hydroxy-1,2, 5-oxadiazole-3-carboxamide	C ₃ H ₅ N ₅ O ₂	143	0.94	\	\
116	N-(2-Hydroxyethyl) hexahydrogen-1H-aceptylamine	C ₈ H ₁₇ NO	143	\	\	0.89
117	2-Methoxy-4-vinyl phenol	C ₉ H ₁₀ O ₂	150	3.08	\	\
118	4-Hydroxy-3-methyl acetophenone	C ₉ H ₁₀ O ₂	150	\	3.48	\
119	4-Ethyl guaiacol	C ₉ H ₁₂ O ₂	152	1.38	2.43	\
120	Vanillin	C ₈ H ₈ O ₃	152	1.02	\	\
121	Isoflavin/isovanillin	C ₈ H ₈ O ₃	152	\	0.11	\
122	2,6-Dimethoxyphenol	C ₈ H ₁₀ O ₃	154	0.46	\	\
123	3,4-Dimethoxyphenol	C ₈ H ₁₀ O ₃	154	\	0.21	\
124	Ethyl 2-heptynoate	C ₉ H ₁₄ O ₂	154	\	0.64	\
125	Valdetamide	C ₉ H ₁₇ NO	155	0.55	\	\
126	Decanal	C ₁₀ H ₂₀ O	156	0.2	\	\
127	Ethyl-2-piperidine formate	C ₈ H ₁₅ NO ₂	157	0.85	\	\
128	4-Butyryl morpholine	C ₈ H ₁₅ NO ₂	157	\	0.54	\
129	2-Hydroxy cyclohexyl ester	C ₈ H ₁₄ O ₃	158	0.26	\	\
130	1,6-Anhydride-B-D-pyran glucose	C ₆ H ₁₀ O ₅	162	6.05	1.05	\
131	1-[(1E)-1-Butenyl]-4-methoxybenzene	C ₁₁ H ₁₄ O	162	0.2	\	\
132	4-Methyl-5-(5-methyl-1H-pyrazol-3-base)-1H-1,2,3-triazole	C ₇ H ₉ N ₅	163	\	0.25	\
133	Eugenol	C ₁₀ H ₁₂ O ₂	164	1.32	1.81	\
134	Cis-isoeugenol	C ₁₀ H ₁₂ O ₂	164	4.96	1.15	\
135	2,3-Dihydro-2,2-dimethyl-7-benzofuranol	C ₁₀ H ₁₂ O ₂	164	0.15	\	\
136	(E)-Isoeugenol	C ₁₀ H ₁₂ O ₂	164	\	5.22	\
137	3-Allyl-6-methoxyphenol	C ₁₀ H ₁₂ O ₂	164	\	0.19	\
138	3,4-Dimethoxystyrene	C ₁₀ H ₁₂ O ₂	164	\	0.1	\
139	Dihydroeugenol	C ₁₀ H ₁₄ O ₂	166	0.41	1.04	\
140	Vanilla ethyl ketone	C ₉ H ₁₀ O ₃	166	0.72	1.08	\
141	4-Methoxy-3-hydroxyacetophenone	C ₉ H ₁₀ O ₃	166	0.33	\	\
142	High vanillin alcohol	C ₉ H ₁₂ O ₃	168	0.44	\	\
143	3-Hydroxyl-4-methoxybenzoic acid	C ₈ H ₈ O ₄	168	0.18	\	\
144	Vanillic acid	C ₈ H ₈ O ₄	168	0.33	\	\
145	6-Hydroxy 5-decanone	C ₁₀ H ₂₀ O ₂	172	0.42	\	\
146	2-Heptyl-1,3-dioxy-amyl ring	C ₁₀ H ₂₀ O ₂	172	\	\	0.29
147	1,3,4-Trimethyl-1,7-dihydrogen-6H-pyrazole and pyridine-6-ketone [3,4-b]	C ₉ H ₁₁ N ₃ O	177	\	0.31	\
148	Coniferyl alcohol	C ₁₀ H ₁₂ O ₃	180	1.96	1	\
149	2,5-Dimethoxyl-4-toluene formaldehyde	C ₁₀ H ₁₂ O ₃	180	0.4	\	\

No.	Name	Molecular formula	Molecular weight	Larch	Area % PBL	UF
150	4-Hydroxyl-3-methoxyphenylacetone	C ₁₀ H ₁₂ O ₃	180	1.07	0.77	\
151	2',4'-Dihydroxyl-3'-methylphenylacetone	C ₁₀ H ₁₂ O ₃	180	\	0.29	\
152	Homovanillic acid	C ₉ H ₁₀ O ₄	182	\	2.15	\
153	Vanillin ethyl ether	C ₁₀ H ₁₄ O ₃	182	1.72	\	\
154	1-Tridecene	C ₁₃ H ₂₆	182	\	0.09	\
155	γ-Dodecane acid lactone	C ₁₁ H ₂₀ O ₂	184	0.71	\	\
156	6-Dodecyl alcohol	C ₁₂ H ₂₆ O	186	\	0.09	\
157	Tetraethylene glycol	C ₈ H ₁₈ O ₅	194	\	\	0.05
158	4-Allyl-2,6-dimethoxyphenol	C ₁₁ H ₁₄ O ₃	194	0.57	0.16	\
159	α-Methyl glucoside	C ₇ H ₁₄ O ₆	194	\	0.21	\
160	2,3-Dimethyl-2-(3-oxobutyl)cyclohexanone	C ₁₂ H ₂₀ O ₂	196	\	0.48	\
161	Ethyl-4-(acetylamino)-1,2,5-oxadiazole-3-carboxylate	C ₇ H ₉ N ₃ O ₄	199	0.53	\	\
162	11-Methyl-12-methylene-tricyclic [5.3.1.1(2,6)]-dodecane-11-alcohol	C ₁₄ H ₂₂ O	206	0.47	\	\
163	Eugenol acetate	C ₁₂ H ₁₄ O ₃	206	0.34	\	\
164	2,5,5,8a-Tetramethylmethyl-4-methylene-4a,5,6,7,8,8a-hexahydrogen-4h-chromene	C ₁₄ H ₂₂ O	206	0.17	\	\
165	Ethyl oxalate	C ₁₁ H ₁₄ O ₄	210	\	0.17	\
166	Tetradecyl alcohol	C ₁₄ H ₃₀ O	214	\	\	0.16
167	10-Oxo-dodecane acid	C ₁₂ H ₂₂ O ₃	214	0.16	\	\
168	3,5-Dimethyl-1-phenyl-1H-pyrazol-4-carboxylic acid	C ₁₂ H ₁₂ N ₂ O ₂	216	0.15	\	\
169	8-Methoxy[1]benzofuran and [3,2-d]pyrimidine -4(3H)-ketone	C ₁₁ H ₈ N ₂ O ₃	216	0.15	0.12	\
170	3,3,4-Trimethyl-4-(4-methylphenyl)cyclopentyl alcohol	C ₁₅ H ₂₂ O	218	0.38	\	\
171	Cubenol	C ₁₅ H ₂₆ O	222	0.28	\	\
172	7-Pentadecanone	C ₁₅ H ₃₀ O	226	\	0.29	\
173	Pentaethylene glycol	C ₁₀ H ₂₂ O ₆	238	\	\	0.52
174	2-(1,3-Dihydrogen-2h-indene-2-subunit)-2,3-dihydrogen-1h-indene-1-ketone	C ₁₈ H ₁₄ O	246	0.18	\	\
175	(Z)-14-Methyl-8-hexadecene-1-acetal	C ₁₇ H ₃₂ O	252	\	0.08	\
176	Palmitic acid	C ₁₆ H ₃₂ O ₂	256	\	0.22	\
177	Dibutyl phthalate	C ₁₆ H ₂₂ O ₄	278	\	0.11	\
178	(13R)-8a,13:9a,13-Diepoxy-15,16-dinorlabdane	C ₁₈ H ₃₀ O ₂	278	0.14	\	\
179	3,4,8-Trimethoxy-6H-benzophenol[c]benzopyran-6-ketone	C ₁₆ H ₁₄ O ₅	286	0.18	\	\
180	1-Naphthalenepropanol, alpha.-ethenyldecahydro-.alpha.,5,5,8a-tetramethyl-2-methylene-, [1S-[1.alpha.(R*),4a.beta.,8a.alpha.]]-	C ₂₀ H ₃₄ O	290	\	0.29	\
181	12-Hydroxyandrostane-17-ketone	C ₁₉ H ₃₀ O ₂	290	0.31	\	\

No.	Name	Molecular formula	Molecular weight	Larch	Area % PBL	UF
182	5,8-Diethoxy-3-(methoxy carbonyl)-2-quinoline carboxylic acid	C ₁₅ H ₁₆ N ₂ O ₆	296	0.36	\	\
183	Di-N-decyl ether	C ₂₀ H ₄₂ O	298	\	0.27	\
184	Vitamin A acetate	C ₂₂ H ₃₂ O ₂	328	\	0.73	\
185	Tetracosane	C ₂₄ H ₅₀	338	\	0.1	\
186	14-Heptacosanone	C ₂₇ H ₅₄ O	394	0.25	\	\
187	Lanosterol	C ₃₀ H ₅₀ O	426	\	0.28	\
188	3',8,8'-Trimethoxy-3-piperidinyl-2,2'-binaphthalene-1,1',4,4'-tetraone	C ₂₈ H ₂₅ NO ₇	487	\	0.34	\

Author details

Liuming Song, Xiao Ge, Xueyong Ren, Wenliang Wang, Jianmin Chang and Jinsheng Gou*

Key Laboratory of Wooden Material Science and Application, College of Materials Science and Technology, Beijing Forestry University, Ministry of Education, Beijing, China

*Address all correspondence to: jinsheng@bjfu.edu.cn

IntechOpen

© 2018 The Author(s). Licensee IntechOpen. This chapter is distributed under the terms of the Creative Commons Attribution License (<http://creativecommons.org/licenses/by/3.0>), which permits unrestricted use, distribution, and reproduction in any medium, provided the original work is properly cited. 

References

- [1] Bridgwater AV, Peacocke GVC. Fast pyrolysis processes for biomass. *Renewable & Sustainable Energy Reviews*. 2000;**4**:1-73. DOI: 10.1016/S1364-0321(99)00007-6
- [2] Mohan D, Pittman CU, Steele PH. Pyrolysis of wood/biomass for bio-oil: A critical review. *Energy & Fuels*. 2006;**20**:848-889. DOI: 10.1021/ef0502397
- [3] Choi SJ, Park SH, Jeon J-K, Lee IG, Ryu C, Suh DJ, et al. Catalytic conversion of particle board over microporous catalysts. *Renewable Energy*. 2013;**54**:105-110. DOI: 10.1016/j.renene.2012.08.050
- [4] Yanik J, Kornmayer C, Saglam M, Yüksel M. Fast pyrolysis of agricultural wastes: Characterization of pyrolysis products. *Fuel Processing Technology*. 2007;**88**:942-947. DOI: 10.1016/j.fuproc.2007.05.002
- [5] Deng N, Zhang Y-F, Wang Y. Thermogravimetric analysis and kinetic study on pyrolysis of representative medical waste composition. *Waste Management*. 2008;**28**:1572-1580. DOI: 10.1016/j.wasman.2007.05.024
- [6] López A, de MI, Caballero BM, Laresgoiti MF, Adrados A. Pyrolysis of municipal plastic wastes: Influence of raw material composition. *Waste Management*. 2010;**30**:620-627. DOI: 10.1016/j.wasman.2009.10.014
- [7] Manzano-Agugliaro F, Alcayde A, Montoya FG, Zapata-Sierra A, Gil C. Scientific production of renewable energies worldwide: An overview. *Renewable and Sustainable Energy Reviews*. 2013;**18**:134-143. DOI: 10.1016/j.rser.2012.10.020
- [8] Han TU, Kim Y-M, Watanabe C, Teramae N, Park Y-K, Kim S, et al. Analytical pyrolysis properties of waste medium-density fiberboard and particle board. *Journal of Industrial and Engineering Chemistry*. 2015;**32**: 345-352. DOI: 10.1016/j.jiec.2015.09.008
- [9] Sheldona RA, Sanders JPM. Toward concise metrics for the production of chemicals from renewable biomass. *Catalysis Today*. 2015;**239**:3-6. DOI: 10.1016/j.cattod.2014.03.032
- [10] Park Y-K, Choi SJ, Jeon J-K, Park SH, Ryoo R, Kim J, et al. Catalytic conversion of waste particle board to bio-oil using nanoporous catalyst. *Journal of Nanoscience and Nanotechnology*. 2012;**12**:5367-5372. DOI: 10.1166/jnn.2012.6412
- [11] Lee HW, Choi SJ, Jeon J-K, Park SH, Jung S-C, Park Y-K. Catalytic conversion of waste particle board and polypropylene over H-beta and HY zeolites. *Renewable Energy*. 2015;**79**: 9-13. DOI: 10.1016/j.renene.2014.07.040
- [12] Kim H, Choi SJ, Kim JM, Jeon J-K, Park SH, Jung S-C, et al. Catalytic copyrolysis of particle board and polypropylene over Al-MCM-48. *Materials Research Bulletin*. 2016;**82**: 61-66. DOI: 10.1016/j.materresbull.2016.03.009
- [13] Jin B-B, Heo HS, Ryu C, Kim S-S, Jeon J-K, Park Y-K. The copyrolysis of block polypropylene with particle board and medium density fiber. *Energy Sources, Part A: Recovery, Utilization, and Environmental Effects*. 2014;**36**: 958-965. DOI: 10.1080/15567036.2010.551263
- [14] Bridgwater AV. Principles and practice of biomass fast pyrolysis processes for liquids. *Journal of Analytical and Applied Pyrolysis*. 1999;**51**:3-22. DOI: 10.1016/S0165-2370(99)00005-4

[15] Babu BV. Biomass pyrolysis: A state-of-the-art review. *Biofuels, Bioproducts and Biorefining: Innovation for a Sustainable Economy*. 2008;2:393-414. DOI: 10.1002/bbb

[16] Zhang Y, He ZB, Xue L, Chu DM, Mu J. Influence of a urea-formaldehyde resin adhesive on pyrolysis characteristics and volatiles emission of poplar particleboard. *RSC Advances*. 2016;6:12850-12861. DOI: 10.1039/c5ra18068f

IntechOpen